



OPEN

SUBJECT AREAS:

POLYMERS

CARBON NANOTUBES AND  
FULLERENESReceived  
23 April 2014Accepted  
24 October 2014Published  
1 December 2014

Correspondence and  
requests for materials  
should be addressed to  
K.H. (kenji-hata@aist.  
go.jp)

\* Current address:  
Department of  
Chemistry, Indian  
Institute of Technology  
Bombay, Powai,  
Mumbai 400076  
(India).

# Influence of matching solubility parameter of polymer matrix and CNT on electrical conductivity of CNT/rubber composite

Seisuke Ata<sup>1,2</sup>, Takaaki Mizuno<sup>2</sup>, Ayumi Nishizawa<sup>2</sup>, Chandramouli Subramaniam<sup>2\*</sup>, Don N. Futaba<sup>1,2</sup> & Kenji Hata<sup>1,2</sup>

<sup>1</sup>Nanotube Research Center, National Institute of Advanced Industrial Science and Technology (AIST), Central5, 1-1-1 Higashi, Tsukuba, Ibaraki 305-8565 (Japan), <sup>2</sup>Technology Research Association for Single Wall Carbon Nanotubes (TASC), 1-1-1 Higashi, Tsukuba, Ibaraki 305-8565, (Japan).

We report a general approach to fabricate elastomeric composites possessing high electrical conductivity for applications ranging from wireless charging interfaces to stretchable electronics. By using arbitrary nine kinds of rubbers as matrices, we experimentally demonstrate that the matching the solubility parameter of CNTs and the rubber matrix is important to achieve higher electrical conductivity in CNT/rubber composite, resulting in continuous conductive pathways leading to electrical conductivities as high as 15 S/cm with 10 vol% CNT in fluorinated rubber. Further, using thermodynamic considerations, we demonstrate an approach to mix CNTs to arbitrary rubber matrices regardless of solubility parameter of matrices by adding small amounts of fluorinated rubber as a polymeric-compatibilizer of CNTs. We thereby achieved electrical conductivities ranging from 1.2 to 13.8 S/cm (10 vol% CNTs) using nine varieties of rubber matrices differing in chemical structures and physical properties. Finally, we investigated the components of solubility parameter of CNT by using Hansen solubility parameters, these findings may useful for controlling solubility parameter of CNTs.

Stretchable devices, such as stretchable circuits, stretchable electronic implants, and flexible displays have emerged as a new paradigm to realize future human-friendly and ubiquitous electronics<sup>1-5</sup>. Indispensable to realizing such devices are stretchable conductive materials, and thus intensive effort have been carried out to introduce conductive functionality to elastomers by the inclusion of electrically conductive fillers. Traditionally, spherical fillers, such as carbon black, have been used<sup>6-8</sup>. However the conductivity realized in Styrene-butadiene rubber (SBR) by the inclusion of over 30 wt% carbon black ( $\sim 10^{-2}$  S/cm) is far from sufficient for applications, such as electrodes of transistor circuits that demand high conductivities ( $10^0\sim 10^2$  S/cm).

Driven by this demand, carbon nanotubes (CNTs) have been considered as a promising substitute for carbon black to realize superior conductive elastomers. In principle, CNTs are excellent fillers, because their high aspect ratio (1000~) and long one-dimensional structure facilitates the formation of conductive pathways throughout the host elastomer matrix. Therefore, higher conductivity has been demonstrated using CNT fillers at lower loading levels compared to spherical fillers. For example, Sekitani et al, used an ionic liquid as a surfactant to mix long single-wall carbon nanotubes<sup>9</sup> (SWCNT) synthesized by water-assisted chemical vapor deposition (CVD) into fluorinated rubber, and achieved 20 S/cm using only a 10 wt% long SWCNT loading<sup>10</sup>. In addition, the significance of this CNT elastomer composited was highlighted by the ability to print it onto a polydimethylsiloxane (PDMS) substrate and demonstrate a conductivity of 90 S/cm to create a stretchable active-matrix display<sup>11</sup>. The key in achieving this high level of conductivity was the use of an ionic liquid as a compatibilizer to enable the dispersion of high aspect SWCNTs into the fluorinated rubber while avoiding phase separation and SWCNT aggregation.

As exemplified, fluorinated rubber is an excellent matrix for highly conductive CNT elastomer composites. However, since the physical and chemical properties of rubber greatly vary with the polymer, the realization of highly conductive CNT rubbers using arbitrary elastomers opens the possibilities for countless applications. For example, in oil sealing, hydrin-, styrene-butadiene-, or acrylonitrile-butadiene-rubber has often been chosen



because of their high durability and resistance to oil. Here, conductivity greater than  $10^{-3} \sim 10^{-2}$  S/cm is required to avoid electrostatic discharge. In similar fashion, when including conductivity on tires for grounding, polybutadiene rubber or acrylic rubber have been used because of their excellent resistance toward weather, exposure to ozone, and wear. Furthermore, for applications that require durability against large deformations, SEBS (hydrogenated polystyrene-*block*-polybutadiene-*block*-polystyrene) and natural rubber (isoprene rubber) have been used because of their high critical and failure strains.

In the past, CNT composite materials employing various non-fluorine based rubbers have been researched; however, the conductivity values ( $\sim 10^{-1}$  S/cm with 10wt% CNT) were vastly inferior compared with that of fluorinated rubber composites ( $\sim 20$  S/cm with 10wt% CNT<sup>12</sup>). For instance, CNTs have been employed as additives for providing conductive functionalities to materials like NBR<sup>13</sup>, SBR and polybutadiene<sup>14</sup>. Specialized techniques, such as double percolation, have been developed to improve the volume conductivities up to  $10^{-1}$  S/cm<sup>15</sup>. However, such techniques are restricted to rubber matrices having good compatibility with CNTs. Thus far, a generalized method for achieving high volume conductivities using CNTs, regardless of the host polymer, like rubbers, elastomer and resins has not been realized.

According to percolation theory, the dispersibility of CNTs is a key factor that determines the ease to form conducting-pathways, and thus a composite with uniformly dispersed CNTs is expected to show higher volume conductivity. Dispersibility of a filler in a matrix can be described by the solubility parameter<sup>16</sup>. Solubility parameter is a well-known parameter that describes the energy required to separate a unit of material or molecules from their neighbors, and thus expresses the degree of interaction between materials. Coleman has introduced the concept of solubility parameter to nano-carbon materials<sup>17</sup>. He demonstrated that carbon nanotubes and graphene could be exfoliated from bundles or graphite to single layers or individuals by using a solvent that minimizes the Gibbs free energy of mixing,  $\Delta G_{\text{mix}}$ . The concept is to choose a solvent that has a similar solubility parameter to that of the nano-carbon material. An apt example is dispersion of HiPCO-SWCNTs into NMP (*N*-methylpyrrolidone), where the solubility parameters were experimentally determined as 20.8 MPa<sup>1/2</sup> and 23.0 MPa<sup>1/2</sup>, respectively to form a spontaneous dispersion of HiPCO-SWCNT. Furthermore, Dixon et al., reported that matching solubility parameter is important to achieve lower percolation threshold and higher mechanical property<sup>18</sup>.

In this article, by using nine diverse varieties of rubbers as matrix, we demonstrated that the highest electrical conductivity of CNT/rubber composites was achieved when the solubility parameters of CNTs and rubber matched, and progressively decreased as the deviation between the solubility parameters increased. Specifically, fluorinated rubber (solubility parameter: 18.5 MPa<sup>1/2</sup>) gave the highest conductivity (13.8 S/cm) because its solubility parameter matched with estimated that of the CNT (solubility parameter: 18.4 MPa<sup>1/2</sup>). We exploited this finding to improve the electrical conductivity of a wide class of rubber matrices with varying solubility parameters by the addition of a small amount of fluorinated rubber as a polymeric-compatibilizer. In this way, the base rubber materials best suited for the application at hand could be chosen without compromising its conductivity.

## Results and Discussion

First, we studied the influence of the matrix rubber on the conductivity by fabricating a series of Super-growth (SG)-SWCNTs rubber composites from an assortment of rubbers, ranging from fluorinated rubber, multi-purpose rubbers (styrene-butadiene rubber (SBR), polybutadiene rubber, isoprene rubber) and specialty rubbers (such as SEBS, Hydrogenated Nitrile Butadiene Rubber (H-NBR), hydrix rubber, acrylic rubber, and Nitrile butadiene rubber (NBR) used in

gaskets and seals). In this work, we used vertically aligned SWCNTs (forests) synthesized by water-assisted chemical vapor deposition<sup>9,16</sup> denoted as “Super-Growth” (SG), to achieve long SWCNTs<sup>19,20</sup>. The SG-SWCNT were qualified as the best available conductive fillers<sup>10–12</sup> because they were very long and thus possessed an exceptionally high aspect ratio, yet were not heavily bundled, and easy to disperse. A suspension of SG-SWCNTs in methyl-isobutyl ketone (MIBK) was dispersed through high pressure jet-milling to create unique, mesh-like SWCNT networks<sup>21</sup>. Various rubbers were added to the dispersion, followed by casting, and MIBK removal to obtain conductive SG-SWCNT/rubber sheets. The SG-SWCNT contents in all such sheets were maintained at 1 vol% and 10 vol% for direct comparison. Conductivities of these sheets showed a strong dependence on the nature of the rubber matrix and ranged from a maximum of  $3.7 \times 10^{-1}$  S/cm for fluorinated rubber to a minimum of  $8.0 \times 10^{-3}$  S/cm for hydrix rubber for 1 vol% SG-SWCNT sheets (Fig. 1a), ranged from a maximum of 13.8 S/cm for fluorinated rubber to a minimum of 1.1 S/cm for SEBS for 10vol% SG-SWCNT sheets (Fig. 1b), in agreement with the trend described in the introduction.

The origin of the variation in conductivity of SG-SWCNT/rubber composites was studied by internal structural observations on ultrathin specimens (thickness: 5  $\mu\text{m}$ ) sliced by a cryo-microtome. SG-SWCNTs within the fluorinated rubber composite (highest conductivity of 13.8 S/cm with 10 vol% SG-SWCNT) showed a well-distributed, highly exfoliated, and interconnected network (Fig. 1c). This indicated the ease of mixing of SG-SWCNTs with fluorinated rubber. In contrast, the SG-SWCNT in SEBS composite (lowest conductivity of 1.1 S/cm with 10 vol% SG-SWCNT), showed a distinct phase-separation and tended to aggregate and form spherical domains, indicating ineffective de-bundling of CNTs and therefore inhomogeneous mixing (Fig. 1d). These results demonstrate the importance of the thorough CNT dispersion in the matrix in determining the conductivity of the SG-SWCNT/rubber composite.

The solubility parameter of SG-SWCNTs was experimentally determined by the dissolution method<sup>22,23</sup>. Here, the solubility parameter of the SG-SWCNTs was experimentally determined as solubility parameter associated with the solvent that exhibited the highest dispersion concentration. SG-SWCNTs were dispersed into 12 solutions of different and known solubility parameters<sup>24</sup> by a high-pressure jet mill followed by ultra-sonication. The solubility parameters are known as Hildebrand solubility parameters  $\delta_T$ <sup>22</sup>. The resultant solutions were stabilized for over 24 hrs. The concentration of the SG-SWCNT in the supernatant of the dispersions was estimated by the Beer-Lambert-Bouguer law<sup>25</sup> based on measured absorbance at 500 nm. Through this process, we could achieve the equilibrium concentrations of the SG-SWCNTs in each of the 12 solutions with different  $\delta_T$ . The concentration was plotted versus the solubility parameters (Fig. 2a). The SG-SWCNT concentration was maximum at a  $\delta_T$  of 18.1 MPa<sup>1/2</sup>, and therefore this value was determined to be the estimated value for SG-SWCNTs. Importantly, this value agreed well with the  $\delta_T$  of fluorinated rubber (18.5 MPa<sup>1/2</sup>). These results demonstrate that the matching between the SG-SWCNT and rubber matrix is one of the crucial aspects to achieve composites possessing superior properties.

We would like to note that the  $\delta_T$  of HiPCO-SWCNTs has been reported as 20.8 MPa<sup>1/2</sup><sup>17</sup>, which is 2.7 MPa<sup>1/2</sup> higher than that of SG-SWCNT. In general, when the  $\delta_T$  of the polymer matrix deviates by greater than two from the filler, the two materials are immiscible. Therefore, SG-SWCNTs and HiPCO SWCNTs are expected to prefer different solvents and matrices. For example,  $\delta_T$  of SG-SWCNT 18.5 MPa<sup>1/2</sup> is close to that of toluene and xylene, and the  $\delta_T$  of HiPCO 20.8 MPa<sup>1/2</sup> is close to that of diphenyl ether and methyl formate. To gain deep insight into the difference of the  $\delta_T$  of SG-SWCNTs and HiPCO-SWCNTs, we decomposed the  $\delta_T$  into Hansen parameters [dispersive-( $\delta_D$ ), polar-( $\delta_P$ ), hydrogen bonding-solubility parameter ( $\delta_H$ )]<sup>26,27</sup>. Since the Hansen parameters of sol-

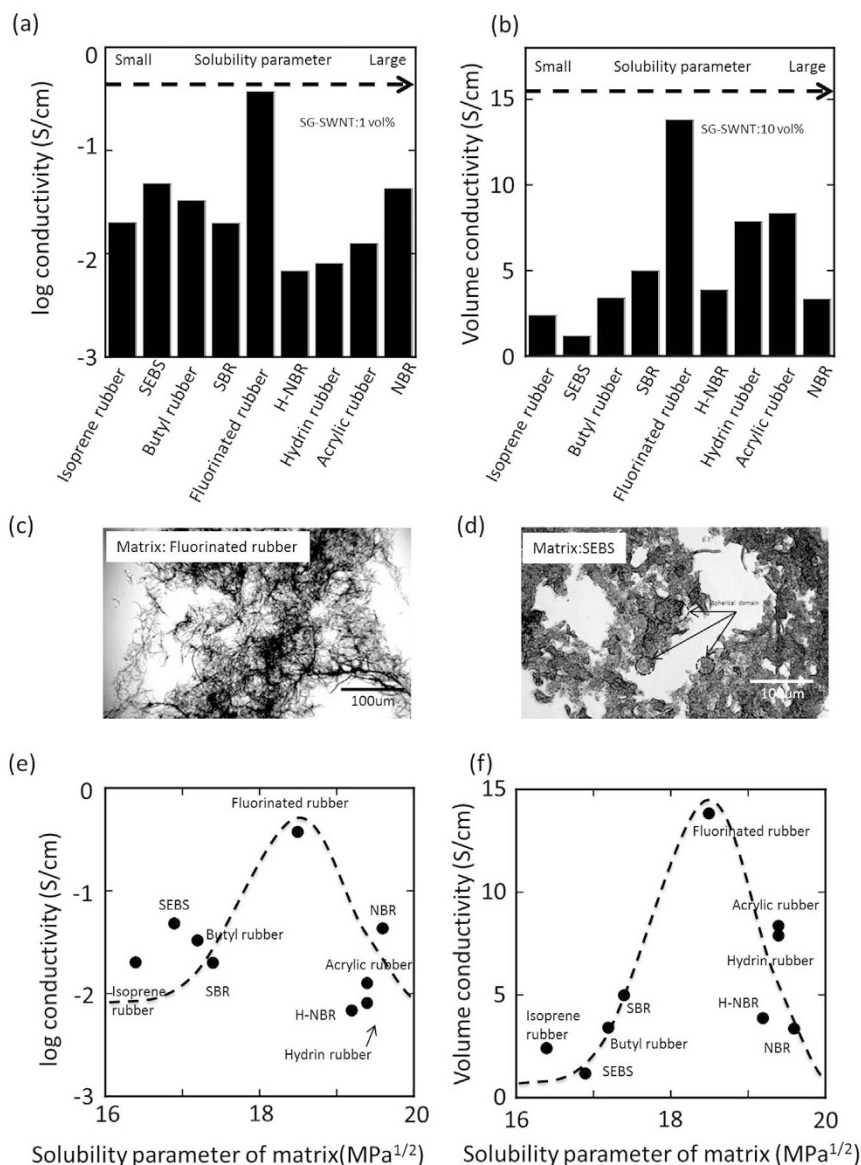


**Figure 1** | (a,b) Volume conductivities of various rubber composites containing 1(a) and 10 vol% (b) SG-SWCNT. (c,d) Optical micrographs of SG-SWCNT morphology in fluorinated rubber (c) and SEBS (d). Ultrathin sections are prepared with cryo-microtoming. Black region is SG-SWCNT and transparent region is rubber.

vents are known (Table 1), we could repeat the process of plotting the equilibrium concentration of SG-SWCNTs versus each Hansen parameter (Fig. 2 b, c, d). For each Hansen solubility parameter, the location of the maximum equilibrium concentration was chosen as the respective Hansen parameter as  $\delta_D = 16.4$ ,  $\delta_P = 7.5$ ,  $\delta_H = 4.0$  MPa<sup>1/2</sup>. When compared to the Hansen parameters of HiPCO-SWCNTs ( $\delta_D = 17.8$ ,  $\delta_P = 7.5$ ,  $\delta_H = 7.6$  MPa<sup>1/2</sup>), we observe a significant difference between  $\delta_D$  and  $\delta_H$ , while  $\delta_P$  was identical. The dispersive Hansen parameter ( $\delta_D$ ), originates from the van der Waals interaction among SWCNTs. Therefore, the dispersive Hansen parameter ( $\delta_D$ ) is expected to decrease with increasing SWCNT diameter; therefore, it is reasonable that the  $\delta_D$  value of the SG-SWCNT ( $d = 3$  nm) is larger than that of HiPCO-SWCNTs ( $d = 1$  nm). The observed identical  $\delta_P$  between the SG-SWCNTs and HiPCO-SWCNT is readily explained because both materials are composed of graphitic carbon and should show identical dipole-dipole interaction. Lastly, at this stage, we cannot provide a conclusive statement regarding the origin between the differences between the  $\delta_H$ . One explanation could be the different levels of

hydrogen functionalization during the dispersion stemming from differences in crystalline defect density.

The volume conductivities of SG-SWCNT/rubber composites were plotted as a function of  $\delta_T$  of the host polymer (Fig. 3a for 1 vol% and Fig. 3b for 10 vol% SG-SWCNT). The highest volume conductivity obtained for SG-SWCNT/fluorinated rubber composite corresponded to a solubility parameter of 18.5 MPa<sup>1/2</sup>. The volume conductivities of all other SG-SWCNT/rubber composites were found to be linearly dependent on the extent of deviation of solubility parameter from 18.5 MPa<sup>1/2</sup>. Thus, we interpret that the solubility parameter to be important in determining the CNT distribution in the matrix and consequently the volume conductivity of the composite.

Based on these findings, we developed a strategy to improve the conductivity of CNT rubbers composite regardless of solubility parameter of matrix, other than fluorinated rubber. Our strategy was to utilize the excellent compatibility of fluorinated rubber with SG-SWCNTs, to other rubber matrices by the addition of 5–10 wt% of fluorinated rubber to the SG-SWCNT rubber composites with the

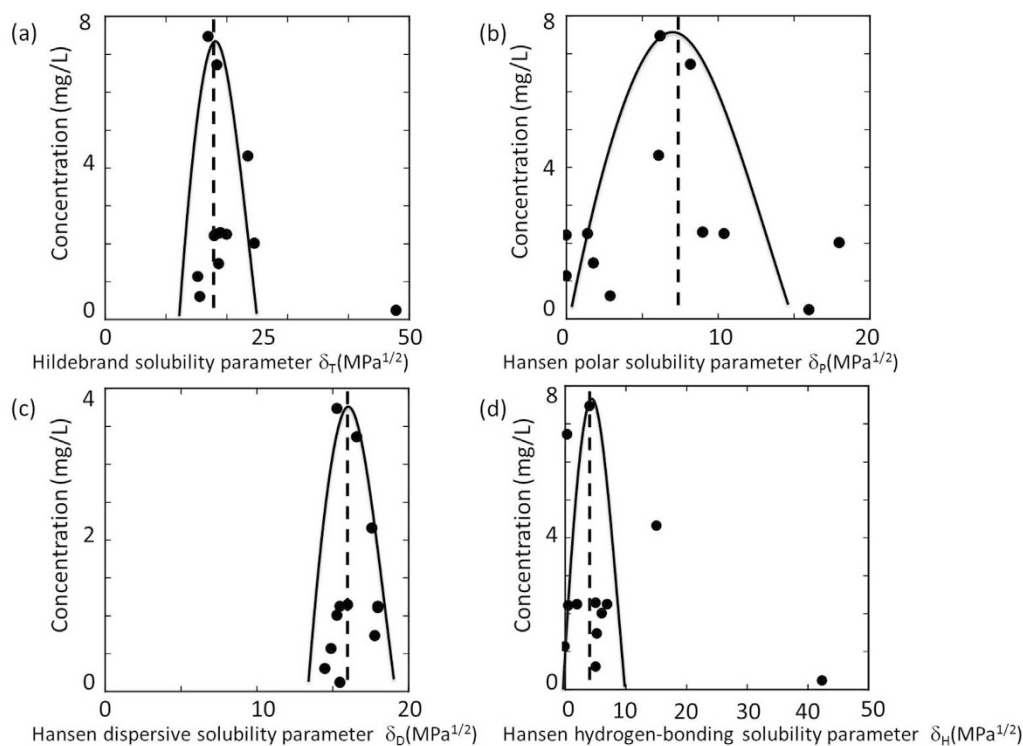


**Figure 2** | SG-SWCNT concentration measured with UV-vis are plotted with solubility parameter of solvent. The solubility parameter peak positions (means calculated solubility parameter of SG-SWCNT) were calculated with statistical method. (a) hildebrand-, (b) polar-, (c) disperse- and (d) hydrogen bonding-solubility parameter.

overall procedure remaining similar as previously described. The composites were thus designated as SG-SWCNT/fluorinated rubber/rubber composites (Fig. 4a, b). To highlight the effect of the fluorinated rubber addition, the volume conductivities of SG-SWCNT/fluorinated rubber/rubber composite samples were compared to those prepared without fluorinated rubber. The results confirmed a distinct improvement in volume conductivities of all such materials prepared using fluorinated rubber as an additive (Fig. 4c, d). Specifically, for a 10 wt% inclusion of fluorinated rubber, the volume conductivities of isoprene rubber, SEBS, polybutadiene rubber, SBR, H-NBR, hydriin and acrylic rubber rubbers showed increases of 1.1 ~ 10 times for 1 vol% SG-SWCNT sheets and increases of 1.5 ~ 3.9 times for 10 vol% SG-SWCNT sheets, respectively. Significantly, the strategy to include a small amount of fluorinated rubber resulted in volume conductivities higher than the targeted 10 S/cm for hydriin rubber and acrylic rubber (Fig. 4d).

Generally, when CNTs are added as filler for composites, the electrical conductivity changes dramatically on an exponential scale

in the region near the percolation threshold. Beyond this region of exponential increase, however, the rate of increase in the conductivity drops, and the addition of more filler does not further enhance the conductivity to any significant degree. For SG-SWCNTs, this percolation threshold is ~0.05 wt%. Here, all of our conductivity results were achieved above this percolation threshold and thus represent values in the saturation regime (1 and 10 wt%). We believe that the factor of ~4 difference in conductivity is significant, since the amount of CNT loading can be reduced by ~4 times, which has a marked impact on practical applications as the intrinsic properties of the matrix can be retained.

Compared to previous reports, the volume conductivities reported here are several times to four-orders of magnitude higher than for the same SWCNT/rubber compositions<sup>28</sup>. Similar improvement in volume conductivities were reported for SBR and BR (from 10<sup>-3</sup> S/cm<sup>7,8</sup> to 8 S/cm), NBR (from 10<sup>-1</sup> S/cm to 8.5 S/cm), SEBS (from 1.0 S/cm to 4.2 S/cm<sup>29</sup>) for 10 vol% SG-SWCNT. Thus, this approach of using a superior filler and fluorinated rubber additive

**Table 1** | SG-SWCNT dispersibility as defined by concentration after dispersion for the solvents used in this work

	$\delta_T$ (MPa <sup>0.5</sup> )	$\delta_P$ (MPa <sup>0.5</sup> )	$\delta_D$ (MPa <sup>0.5</sup> )	$\delta_H$ (MPa <sup>0.5</sup> )	Concentration(mg/L)
n-hexane	15.3	0.0	14.9	0.0	1.1
diethyl ether	15.6	2.9	14.5	5.1	0.6
methyl isobutyl ketone	17.0	6.2	15.3	4.1	7.5
1,3,5-trimethylbenzene	18.0	0.0	18.0	0.6	2.2
toluene	18.2	1.4	18.0	2.0	2.2
1,1-dichloroethane	18.4	8.2	16.6	0.4	6.7
fran	18.7	1.8	17.8	5.3	1.5
MEK	19.0	9.0	16.0	5.1	2.3
acetone	20.0	10.4	15.5	7.0	2.2
isopropanol	23.5	6.1	17.6	15.1	4.3
acetonitrile	24.6	18.0	15.3	6.1	2.0
water	47.9	16.0	15.5	42.4	0.2

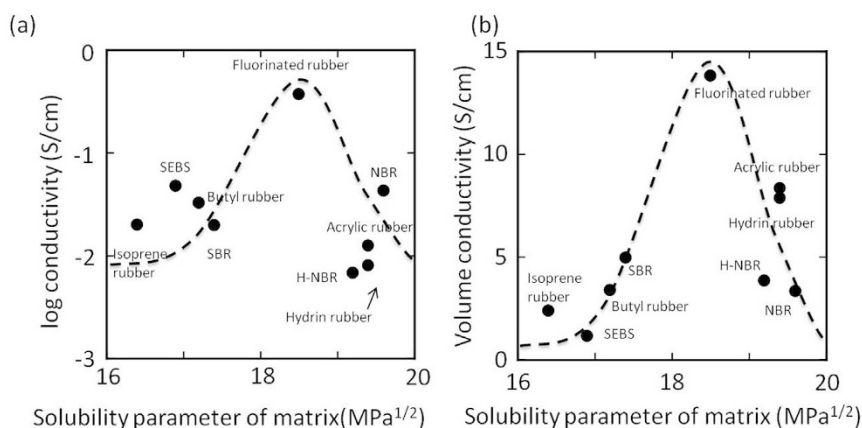


**Figure 3** | Volume conductivities of SG-SWCNT/rubber sheets versus solubility parameter of respective matrices (rubber). (a) and (b) indicate results of 1 and 10 vol% SG-SWCNT, respectively.

was successful in achieving significant improvement in the volume conductivities. Therefore, this generalized strategy is expected to significantly broaden the choices for host polymers and widen the scope of applications for conductive rubbers.

In order to elucidate the effect of solubility parameter on the conductivity improvement of SG-SWCNT (1 vol% and 10 vol%)/fluorinated rubber/rubber composites, a plot of  $\delta_{HP}$  (solubility parameter of host polymer) versus the corresponding volume conductivities was constructed for two different fluorinated rubber fractions (5 and 10 wt%) (Fig. 4e, f). In addition to the improvement in conductivity described above, a corresponding difference in solubility parameter between rubber and fluorinated rubber, with a larger deviation of  $\delta_{HP}$  from  $\delta_{FR}$  (solubility parameter of fluorinated rubber) giving rise to greater conductivity enhancements was observed. Cross-sectional scanning electron microscopy (SEM) images showed that SG-SWCNT appeared to be well-dispersed and distributed uniformly throughout the composite for SG-SWCNT/fluorinated rubber (10 vol%)/SEBS (Fig. 5a), in sharp contrast to the same composite without fluorinated rubber that showed wide-spread phase separation of the CNTs and rubber (Fig. 1d).

Further structural characterizations were carried out to investigate how fluorinated rubber contributed to improving the volume conductivity. SEM (Fig. 5b) and energy-dispersive X-ray (EDX) spectroscopic elemental mapping (Fig. 5c) showed that fluorinated rubber was not uniformly distributed and that phase separation had occurred resulting in domains with a large quantity of fluorinated rubber and isoprene rubber (Fig. 5c). In order to assess the distribution of CNT in the EDX image, Raman spectral mapping based on SG-SWCNT G-band intensity was carried out in the same location with each pixel of the map representing an area of 25  $\mu\text{m}^2$ . This G-band (at  $\sim 1590\text{ cm}^{-1}$ ) due to the graphitic structure of CNT could be observed for CNT encapsulated in rubber matrices (Fig. 5e). With fluorinated rubber and isoprene rubber lacking a prominent G-band (Fig. 5e), the G-band intensity provided a unique signature to track the distribution of CNTs. Overlapping the spectral and elemental maps showed a strong G-band intensity in the fluorinated rubber-rich regions and a relatively weak G-band intensity for the isoprene-rich regions (Fig. 5f). Thus, the SG-SWCNT concentration was shown to be higher in fluorinated rubber regions. These results agreed with the strong affinity of SG-SWCNTs with the fluorinated rubber resulting in the SG-SWCNTs preferentially gathering in the domains of fluorinated rubber. We interpret that such preferential localization of SG-SWCNT in the fluorinated rubber domains led to increased contact and overlapping between SG-SWCNTs within the domain. We note that we have observed that when amount of fluorinated rubber, which is added to the host matrix, is too low, a continuous network of CNTs could not be made throughout rubber, and

therefore the advantage was lessened. It is reasonable that if the amount of fluorinated rubber is significantly raised beyond our levels, the inherent properties of the host matrix would degrade.

The experimental finding of the linear increase in volume conductivity to the deviation of  $\delta_{HP}$  from  $\delta_{FR}$  (18.5 MPa<sup>1/2</sup>) can be understood from the addition of fluorinated rubber. The larger deviation in the  $\delta_{HP}$  for the  $\delta_{CNT}$  and the  $\delta_{FR}$ , the poorer the affinity of SG-SWCNTs with the host polymer. Therefore, the SG-SWCNTs preferentially mixed into the regions of fluorinated rubber to create islands of well de-bundled CNTs. Due to the length of the SG-SWCNTs, these islands were connected by CNT bundles bridges the interstitial regions thereby creating a network structure spanning the entire macroscopic structure. As a result, the density of contacts between individual SG-SWCNTs, and therefore between fluorinated rubber domains, improves volume conductivity. Due to this important effect, the conductivity of the composites (at 10 wt% fluorinated rubber) could be raised to  $\sim 10\text{ S/cm}$  regardless of the rubber matrices.

In conclusion, we demonstrated that matching solubility parameter is important to achieve higher conductivity in CNT rubber composite by using nine kinds of rubbers as matrices. Based on these findings, we propose that the addition of a small amount of fluorinated rubber into the rubber matrix as a general and practical approach to improve the conductivity of arbitrary CNT/rubber composites.

Such SG-SWCNT/rubber composites presented here, possesses additional advantages such as excellent mechanical durability originating from the ability of long and traversing SWCNTs to deform in concert with the elastomer with minimum stress concentration at their interfaces. Finally, we note that the SG-SWCNT synthetic technology has been successfully scaled-up to a pilot production plant where large growth substrates are continuously conveyed through the reactor enabling annual ton-scale SWCNT production for the first time. Combined with the results of this work, we envision the realization of versatile applications for CNT rubber with various rubber matrices such as, stretchable electronics, flexible displays, and automobile parts.

## Methods

We used super-growth SWCNTs ( $>99.98\%$  in purity,  $>1\text{ mm}$  in length, and  $3\text{ nm}$  in diameter) unless otherwise specified. Millimeter-scale tall SWCNT (SG-SWCNT) forests were synthesized from iron catalyst nano particles on a Ni alloy metal substrate<sup>17</sup> using ethylene as the carbon feedstock and water as a growth enhancer. Purity of SG-SWCNT is more than 99.5% which was measured by thermogravimetric analysis (Figure S1). Typically, we mixed the SWCNTs in MIBK 4-methyl-2-pentanone (8 ml) for 12 h. A suspension of SG-SWCNTs in methyl-isobutyl ketone (MIBK) was dispersed through high pressure jet-milling (100 MPa and 120 MPa, Sugino Machine, Japan) to create unique, mesh-like SWCNT networks<sup>21</sup>. The mixture was stirred at 80 °C for 24 hour to remove the MIBK and the resulting gel-like

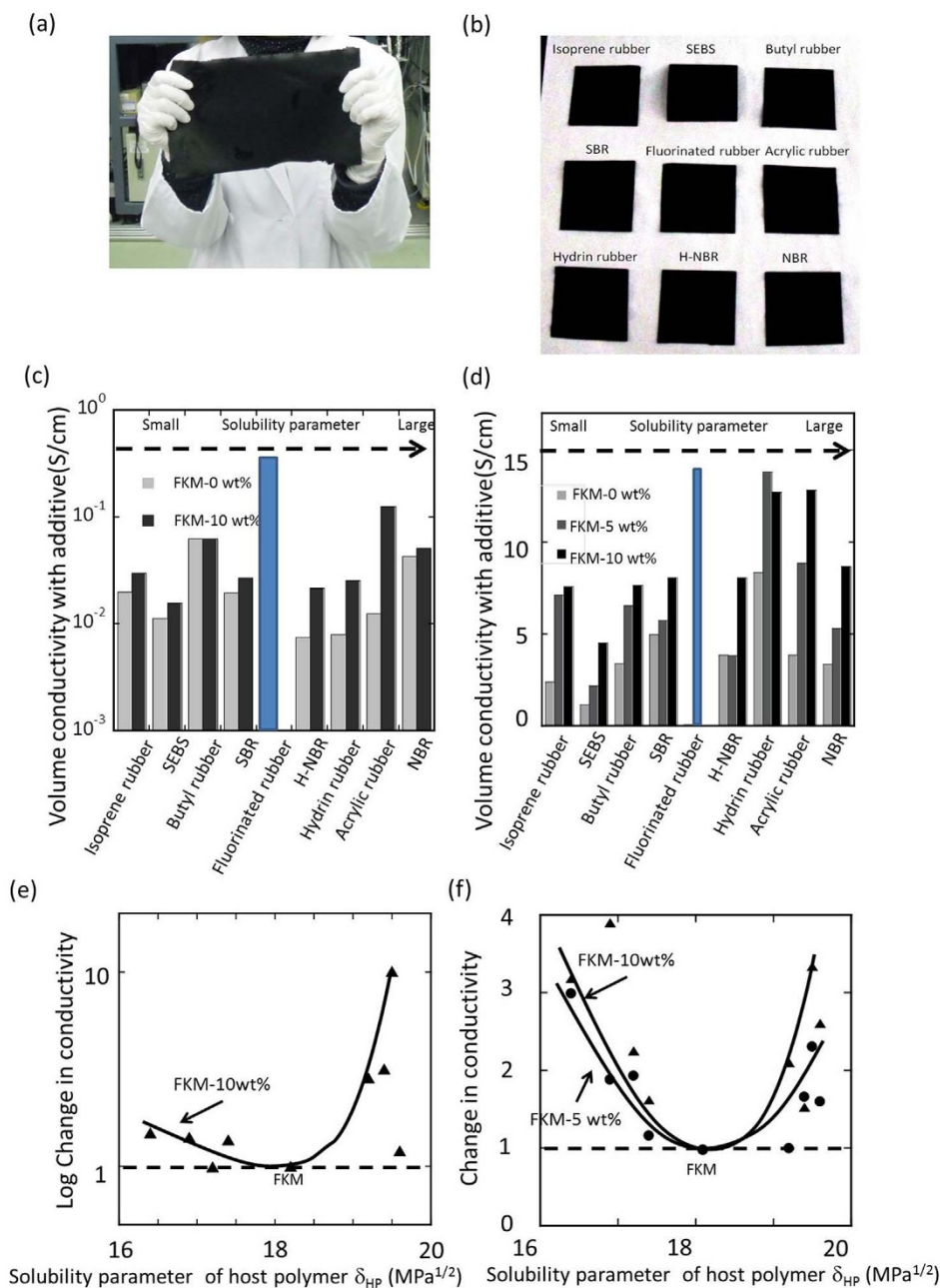


**Figure 4** | (a, b) Photograph showing an A4 scale SG-SWCNT/fluorinated rubber (10 vol%)/isoprene-rubber composite (a) and SG-SWCNT/elastomers with fluorinated rubber as additive (b). (c, d) Volume conductivity change with adding 5 and 10 wt% fluorinated rubber. (c) and (d) indicate 1 and 10 vol% SG-SWCNT, respectively. (e, f) Change in conductivities (conductivity with fluorinated rubber divided by conductivity without fluorinated rubber) versus solubility parameter of host polymer.

solution was poured onto a glass plate by drop casting and then air-dried for 24 hours to obtain a composite film. The SG-SWCNT contents in all such sheets were maintained at 1 vol% and 10 vol% for direct comparison. Volume conductivities of sheets measured by using Van der Pauw 4-terminal method using a MCP-T610 and MCP-TPLSP probe (Mitsubishi Chemical Analytech Co., LTD). Rubbers were added to the SG-SWCNT solution. The following are details of rubbers used in this manuscript; SBR (Nipol1502. Styrene fraction is 23.5%. Calculated  $\delta$  is 17.4 MPa<sup>1/2</sup>), butyl rubber (Nipol BR1220. Mooney viscosity is 44 ML. Calculated  $\delta$  is 17.2 MPa<sup>1/2</sup>), isoprene rubber (Nipol IR 2200. Mooney viscosity is 82 ML. Calculated  $\delta$  is 16.4 MPa<sup>1/2</sup>), NBR (Nipol DN3350. Fraction of acrylonitrile is 33%. Calculated  $\delta$  is 19.6 MPa<sup>1/2</sup>), HNBR (Zetpol 2020. Fraction of acrylonitrile is 36.2%, iodine value is 28 mg/100 mg. Calculated  $\delta$  is 19.2 MPa<sup>1/2</sup>), hydrin rubber (Hydrin T3106. Mooney viscosity is 60 ML. Calculated  $\delta$  is 18.2 MPa<sup>1/2</sup>), acryl rubber (Nitpol AR 12. Mooney viscosity is 33 ML. Calculated  $\delta$  is 19.4 MPa<sup>1/2</sup>) were purchased from Zeon Corporation, Japan. Fluorinated rubber (DAI-EL G 912, which comprising terpolymer of vinylidene fluoride, tetrafluoroethylene and hexafluoropropylene. Fluorine contents are 70.5 wt%.  $\delta$  is

18.5 MPa<sup>1/2</sup>) was purchased from Daikin Industries, Ltd. Solubility parameters of rubbers were calculated by the Group Contribution Method<sup>30</sup>.

CNT morphology in rubbers were observed by digital microscope after making ultra-thin sections ( $t=5$   $\mu\text{m}$ ) with cryo-microtome (RM2265, Leica, at  $-80^\circ\text{C}$ ). Raman shift spectrum measurement and their mapping were carried out by Raman spectrometer (Nicolet Almega XR, Thermo Fischer Scientific Inc.) with laser excitation at a wavelength of 532 nm. Energy dispersive X-ray spectrometry (EDX) measurement was carried out with EDX analyzer (X Flash 6/30, Bruker) attached on scanning electron microscope (S4800, Hitachi). Determine solubility parameter SG-SWCNTs were dispersed into 12 kinds of different and known solubility parameters by a high-pressure jet mill (100 and 120 MPa, 2 passes, HJP17004, Sugino Machine Co.) follow by ultra-sonication ( $W = 600$  W, 24 kHz, 1 h,  $40^\circ\text{C}$ ). The resultant solutions were stabilized for over 24 hrs. The concentration of the SG-SWCNT in the supernatant of the dispersions were estimated by the Beer-Lambert-Bouguer law (specific extinction coefficient for SG-SWCNT of  $\epsilon_{500} = 2.06 \times 10^4$  cm<sup>2</sup>g<sup>-1</sup>) based on measured light absorbance at 500 nm (UV-3600, Shimadzu Co.)<sup>25</sup>.

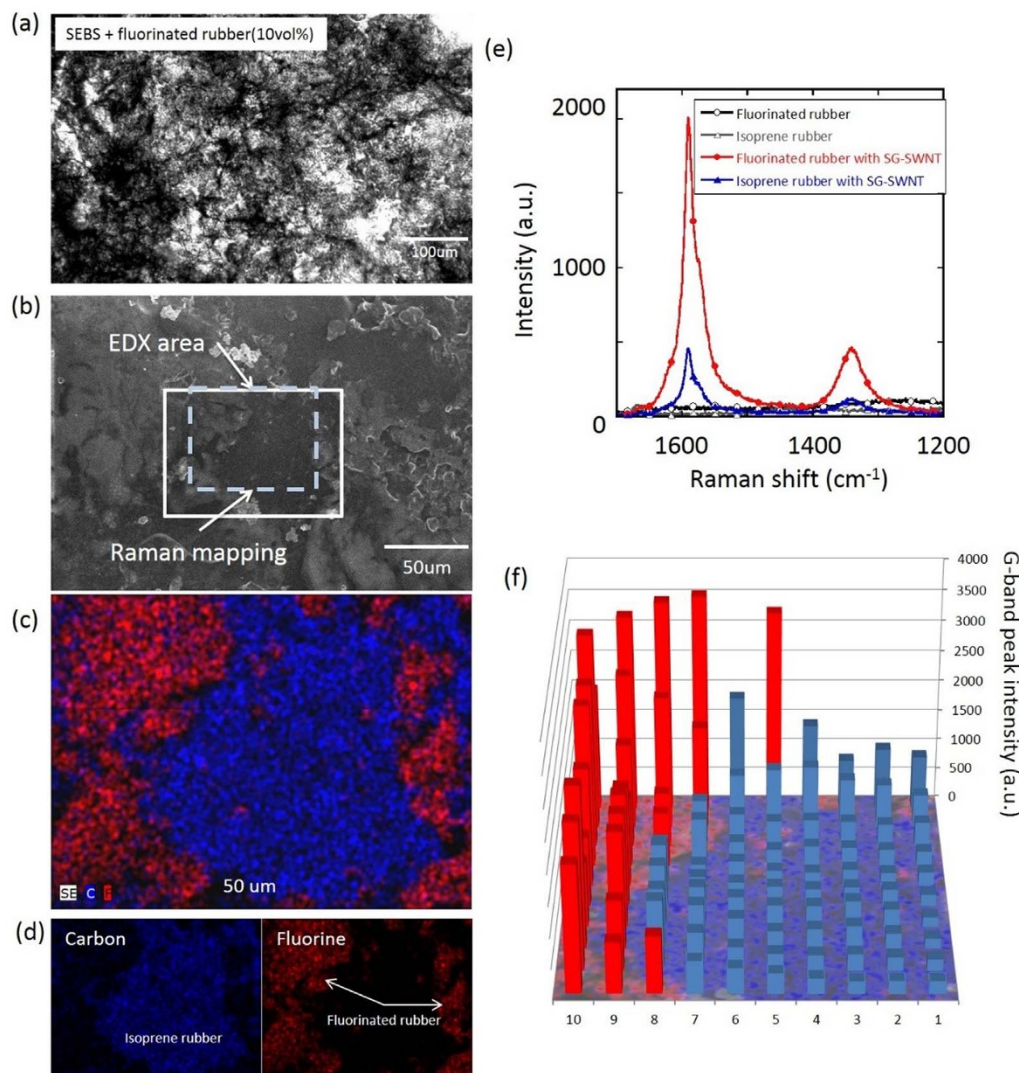


**Figure 5** | (a) SG-SWCNT morphology in SEBS with 10 vol% fluorinated rubber (b) Cross-sectional SEM image of SG-SWCNT/fluorinated rubber (10 vol%)/isoprene rubber. The region within the white box is used for EDX spectral mapping based on intensities of Carbon and Fluorine and their combination (d). The area is used for Raman mapping. (e) Raman spectrum of pure rubbers and SG-SWCNT in rubbers. (f) G-band intensities at square region in (b).

Hansen solubility parameter is defined as follows,

$$\delta^2 = \sqrt{\delta_D^2 + \delta_P^2 + \delta_H^2}, \quad (1)$$

where,  $\delta_D$ ,  $\delta_P$ ,  $\delta_H$  represent the strength of dispersive-, polar- and hydrogen bonding interactions, respectively<sup>26,27</sup>.

- Lacour, S. P., Jones, J., Suo, Z. & Wanger, S. Design and performance of thin metal interconnects for skin-like electronic circuits. *IEEE Electron Device Lett.* **25**, 179–181 (2004).
- Brosteaux, D., Axisa, F., Gonzalez, M. & Vanfleteren, J. Design and Fabrication of Elastic Interconnections for Stretchable Electronic Circuits. *IEEE Electron Device Lett.* **28**, 552–554. (2007)
- Khang, D., Jiang, H., Huang, Y. & Rogers, J. A Stretchable Form of Single-Crystal Silicon for High-Performance Electronics on Rubber Substrates. *Science* **311**, 208–2112 (2006).
- Rogers, J., Someya, T. & Huang, Y. Materials and mechanics for stretchable electronics. *Science* **327**, 1603–1607 (2010).
- Sekitani, T. & Someya, T. Stretchable, Large-area Organic Electronics. *Advanced Materials* **22**, 20, 2228–2246 (2010).
- Karasek, L. & Sumita, M. Characterization of dispersion state of filler and polymer-filler interactions in rubber-carbon black composites. *J. Materials Science* **31**, 2, 281–289 (1996).
- Tchoudakov, R., Breuer, O., Narkis, M. & Siegmann, A. Conductive polymer blends with low carbon black loading: Polypropylene/polyamide. *Polymer Engineering and Science* **36**, 10, 1336–1346 (1996).
- Das, N., Chaki, T. & Khastgir, D. Effect of processing parameters, applied pressure and temperature on the electrical resistivity of rubber-based conductive composites. *Carbon* **40**, 6, 807–816 (2002).
- Hata, K. *et al.* Water-assisted highly efficient synthesis of impurity-free single-walled carbon nanotubes. *Science* **306**, 1362–1364 (2004).
- Sekitani, T. *et al.* A Rubberlike Stretchable Active Matrix Using Elastic Conductors. *Science* **321**, 1468–1472 (2008).
- Sekitani, T. *et al.* Stretchable active-matrix organic light-emitting diode display using printable elastic conductors. *Nature Materials* **8**, 494–499 (2009).
- Ata, S., Kobashi, K., Yumura, M. & Hata, K. Mechanically Durable and Highly Conductive Elastomeric Composites from Long Single-walled Carbon Nanotubes Mimicking the Chain structure of Polymers. *Nano Letters* **12**, 6, 2710–2716 (2012).
- Verge, P., Peeterbroeck, S., Bounnaud, L. & Dubois, P. Investigation on the dispersion of carbon nanotubes in nitrile butadiene rubber: Role of polymer-to-filler grafting reaction. *Composites Science and Technology* **70**, 10, 1453–1459 (2010).
- Das, A. *et al.* Coupling activity of ionic liquids between diene elastomers and multi-walled carbon nanotubes. *Carbon* **47**, 14, 3313–3321 (2009).
- Li, Y. & Shimizu, H. Conductive PVDF/PA6/CNTs nanocomposites fabricated by dual formation of cocontinuous and nanodispersion structures. *Macromolecules* **41**, 14, 5339–5344 (2008).
- Hildebrand, J. *The Solubility of Non-Electrolytes* [Hamor, A. (ed.)][268](Reinhold Publishing Corp., New York, 1936).
- Bergin, S. D. *et al.* Multicomponent Solubility Parameters for Single-Walled Carbon Nanotube–Solvent Mixtures. *ACS NANO* **3**, 8, 2340–2350 (2009).



18. Dooher, T. & Dixon, D. Multiwalled Carbon Nanotube/Polysulfone Composites: Using the Hildebrand Solubility Parameter to Predict Dispersion. *Polymer Composites* **32**, 1895–1903 (2011).
19. Futaba, D. N. *et al.* 84% Catalyst Activity of Water Assisted Growth, Single Walled Carbon Nanotube Forest Characterization by a Statistical and Macroscopic Approach. *J. Phys. Chem. B* **110**, 15, 8035–8038 (2006).
20. Mizuno, K. *et al.* Selective Matching of Catalyst Element and Carbon Source in Single-Walled Carbon Nanotube Synthesis on Silicon Substrates. *J. Phys. Chem. B* **109**, 7, 2632–2637 (2005).
21. Kobashi, K. *et al.* A Dispersion Strategy: Dendritic Carbon Nanotube Network Dispersion for Advanced Composites. *Chemical Science* **4**, 2, 727–733 (2013).
22. Launay, H. Hansen, C. & Almdal, K. Hansen solubility parameters for a carbon fiber/epoxy composite. *Carbon* **45**, 2859–2865 (2007).
23. Ma, J. & Zhou, L. A new procedure for calculating Hansen solubility parameters of carbon nanotube/polymer composites. *Polym. Bull.* **68**, 1053–1063 (2012).
24. Brandrup, J., Immergut, E. H. & Grulke, *Polymer hand book 4th ed.* [VII675–711] (Wiley-Inter science, New York, 1999).
25. Jeong, S. *et al.* Optical absorption spectroscopy for determining carbon nanotube concentration in solution. *Synthetic Metals* **157**, 570–574 (2007).
26. Hansen, C. M. & Skaarup, K. The Three Dimensional Solubility Parameter - Key to Paint Component Affinities III. - Independent Calculation of the Parameter Components. *J. Paint Tech.* **39**, 511–514 (1967).
27. Hansen, C. *Hansen Solubility Parameters: A User's Handbook, Second Edition* [Hansen, C. (ed.)][4–5](CRC Press, 2007).
28. Bauhofer, W. & Kovacs, A review and analysis of electrical percolation in carbon nanotube polymer composites. *J. Composites Science and Technology* **69**, 10, 1486–1498 (2009).
29. Li, Y. & Shimizu, H. Toward a Stretchable, Elastic, and Electrically Conductive Nanocomposite: Morphology and Properties of Poly[styrene-*b*-(ethylene-*co*-butylene)-*b*-styrene]/Multiwalled Carbon Nanotube Composites Fabricated by High-Shear Processing. *Macromolecules* **42**, 7, 2587–2593 (2009).
30. Elbro, H., Fredenslund, A. & Rasmussen, P. Group contribution method for the prediction of liquid densities as a function of temperature for solvents, oligomers, and polymers. *I&EC research* **30**, 2576–2582 (1991).

## Acknowledgments

We gratefully acknowledge Dr. Kazufumi Kobashi and Dr. Shunsuke Sakurai for useful discussions. Supported by Technology Research Association for Single Wall Carbon Nanotubes are acknowledged. This paper is based on results obtained from a project commissioned by the New Energy and Industrial Technology Development Organization (NEDO).

## Author contributions

S.A. designed the experiments and discussed the results. T.M. and A.N. conducted the experiments and collected all data. C.S. and D.F. discussed the results and helped in drafting the manuscript. K.H. supervised the overall research and conceived the initial idea of the experiments.

## Additional information

**Supplementary information** accompanies this paper at <http://www.nature.com/scientificreports>

**Competing financial interests:** The authors declare no competing financial interests.

**How to cite this article:** Ata, S. *et al.* Influence of matching solubility parameter of polymer matrix and CNT on electrical conductivity of CNT/rubber composite. *Sci. Rep.* **4**, 7232; DOI:10.1038/srep07232 (2014).



This work is licensed under a Creative Commons Attribution-NonCommercial-NoDerivs 4.0 International License. The images or other third party material in this article are included in the article's Creative Commons license, unless indicated otherwise in the credit line; if the material is not included under the Creative Commons license, users will need to obtain permission from the license holder in order to reproduce the material. To view a copy of this license, visit <http://creativecommons.org/licenses/by-nc-nd/4.0/>